Journal of Alloys and Compounds 506 (2010) 600–606

Contents lists available at ScienceDirect

Journal of Alloys and Compounds

journal homepage: www.elsevier.com/locate/jallcom

Mechanical property retention in remelted microparticle to nanoparticle AZ31/Al_2O_3 composites

M. Paramsothy[a], Q.B. Nguyen[a], K.S. Tun[a], J. Chan[b], R. Kwok[b], J.V.M. Kuma[c], M. Gupta[a,*]

[a] Department of Mechanical Engineering, National University of Singapore, 9 Engineering Drive 1, Singapore 117576, Singapore
[b] Singapore Technologies Kinetics Ltd. (ST Kinetics), 249 Jalan Boon Lay, Singapore 619523, Singapore
[c] Minerals, Metals & Materials Technology Centre, National University of Singapore, 9 Engineering Drive 1, Singapore 117576, Singapore

ARTICLE INFO

Article history:
Received 18 May 2010
Received in revised form 14 July 2010
Accepted 15 July 2010
Available online 22 July 2010

Keywords:
AZ31/Al_2O_3 composites
Remelting
Mechanical properties

ABSTRACT

In this work, three AZ31/Al_2O_3 composites were synthesized and remelted using the disintegrated melt deposition solidification processing technique. Al_2O_3 particles of 50 nm, 300 nm and 1000 nm sizes were individually used to formulate the composites of 1.5 vol%, 5.0 vol% and 10.0 vol% reinforcement content, respectively. In each case after extrusion, the change in microstructure and mechanical properties before and after remelting was not significant. Given the strong affinity Mg has for oxygen from the Al_2O_3 particle, the insignificant change in mechanical properties indicated the friendly nature of AZ31/Al_2O_3 composites towards initial remelting. In particular, compared to the submicron and micron particle reinforced composites of limited tensile ductility, the nanoparticle reinforced composite retained its significantly higher tensile ductility (up to +400% more) after the initial remelting.

1. Introduction

AZ31 is an Al-containing (or Zr-free) Mg alloy which is commonly used in weight-critical structural applications in the automotive, aerospace and marine industries. It is characterized by: (a) low cost, (b) ease of handling, (c) good strength and ductility and (d) resistance to atmospheric corrosion. AZ31 has been surface-reinforced with SiC microparticulates [1], C_{60} molecules [2], and multi-walled carbon nanotubes [3] using the friction stir processing technique, recently. Good dispersion and hardening of the base matrix at the surface were reported in these studies. In the case of AZ31/SiC microcomposite, defect-free and adherent particle–matrix interface has been reported [4–6]. TiNi shape memory alloy (SMA) fibers have been incorporated in AZ31 matrix using pulsed current hot pressing (PCHP) [7]. Here, there was no significant interfacial reaction. The yield stress and elongation in the AZ31/TiNi microcomposite increased with temperature, strength significantly exceeding that of the AZ31 matrix, due to residual compressive stress in the AZ31 matrix based on phase change induced shrinkage of the TiNi fiber. Recently, carbon nanotubes have been used for simultaneously improving tensile strength and ductility of AZ31 [8]. Also, researchers added Al_2O_3 nanoparticles to AZ31 using disintegrated melt deposition (DMD) and synthesized nanocomposites [9–12]. Tensile strength and ductility of AZ31 have been simultaneously and significantly increased with the use of Al_2O_3 nanoparticles as well [12]. In any metal solidification processing operation, remelting plays an important role in reconsolidation of the metal-based material. This is primarily for reuse of the original material for cost-cutting and environmentally friendly reasons [13]. Reuse of the original material consumes only a fraction of the energy required to produce the same material from scratch (therefore lowering cost and harm to the environment) [14]. In the case of metal matrix composites where there can be significant metal–ceramic reactivity, a major concern is the deterioration of mechanical properties due to remelting [14–16], independent of unacceptably high levels of impurities such as inclusions, oxides and hydrogen gas [17]. However, open literature search has revealed that no successful attempt has been made to retain or improve the tensile strength and ductility (after extrusion) of any AZ31 nanocomposite after remelting.

Accordingly, one of the primary aims of this study was to at least retain the tensile strength and ductility (after extrusion) of an AZ31/Al_2O_3 nanocomposite after initial remelting. Another parallel aim of the present study was to evaluate the initial remelting effects (after extrusion, if any) pertaining to AZ31 composites individually containing submicron or micron sized Al_2O_3 particle reinforcement. DMD followed by hot extrusion was used to synthesize the AZ31/Al_2O_3 composites.

2. Experimental procedures

2.1. Materials

In this study, AZ31 ingot (nominally 2.50–3.50 wt% Al, 0.60–1.40 wt% Zn, 0.15–0.40 wt% Mn, 0.10 wt% Si, 0.05 wt% Cu, 0.01 wt% Fe, 0.01 wt% Ni, balance Mg) supplied by Tokyo Magnesium Co. Ltd. (Yokohama, Japan) was used as the matrix

* Corresponding author. Tel.: +65 6516 6358; fax: +65 6779 1459.
E-mail address: mpegm@nus.edu.sg (M. Gupta).

0925-8388/$ – see front matter © 2010 Elsevier B.V. All rights reserved.
doi:10.1016/j.jallcom.2010.07.123

material. AZ31 block was sectioned to smaller pieces. All oxide and scale surfaces were removed using machining. All surfaces were washed with ethanol after machining. All Al_2O_3 particles (50 nm, 300 nm and 1000 nm sizes) supplied by Baikowski (Japan) were used as reinforcement phases.

2.2. Processing

Monolithic AZ31 was cast using the DMD method [9,10]. This involved heating AZ31 pieces to 750 °C in an inert Ar gas atmosphere in a graphite crucible using a resistance-heating furnace. The crucible was equipped with an arrangement for bottom pouring. Upon reaching the superheat temperature, the melt was stirred for 5 min at 460 rpm using a twin blade (pitch 45°) mild steel impeller to facilitate the uniform distribution of heat. The impeller was coated with Zirtex 25 (86% ZrO_2, 8.8% Y_2O_3, 3.6% SiO_2, 1.2% K_2O and Na_2O, and 0.3% trace inorganics) to avoid iron contamination of the molten metal. The melt was then released through a 10-mm diameter orifice at the base of the crucible. The melt was disintegrated by two jets of argon gas oriented normal to the melt stream and located 265 mm from the melt pouring point. The argon gas flow rate was maintained at 25l pm. The disintegrated melt was subsequently deposited onto a metallic substrate located 500 mm from the disintegration point. An ingot of 40 mm diameter was obtained following the deposition stage. To form the fresh ingots of AZ31/Al_2O_3 composites, Al_2O_3 particle powder was placed in alternating layers with AZ31 pieces with all other DMD parameters unchanged. All deposited fresh ingots were sectioned into billets partly for extrusion (described below) with the remainder of the billets remelted once with all other DMD parameters unchanged. Prior to remelting, (a) all oxide and scale surfaces of the billets were removed using machining and (b) all surfaces of the billets were washed with ethanol after machining. Remelted ingots of AZ31/Al_2O_3 composites were obtained in this way and also sectioned into billets for extrusion.

All billets from fresh and remelted ingots were machined to 35-mm diameter and hot extruded using 20.25:1 extrusion ratio on a 150 ton hydraulic press. The extrusion temperature was 350 °C. The billets were held at 400 °C for 60 min in a furnace prior to extrusion. Colloidal graphite was used as a lubricant. Rods of 8 mm were obtained.

The content of 50 nm, 300 nm and 1000 nm sized Al_2O_3 particle reinforcements used in the AZ31/Al_2O_3 composites was 1.5 vol%, 5.0 vol% and 10.0 vol%, respectively. These contents were selected primarily for achieving significant increase in strength of AZ31 based on critical volume fraction of particle reinforcement [12,14]. If the relatively lowest 1.5 vol% Al_2O_3 particle content was used in formulating the submicron and micron AZ31/Al_2O_3 composites, there would most likely not have been a significant increase in strength of AZ31.

2.3. Microstructural characterization

Microstructural characterization studies were conducted on metallographically polished monolithic and composite extruded samples to determine grain characteristics and Al_2O_3 reinforcement distribution. Hitachi S4300 Field-Emission Scanning Electron Microscope (FESEM) was used for observing Mg grains and Al_2O_3 particles. Image analysis using Scion software was carried out to determine the grain size.

2.4. X-ray diffraction studies

X-ray diffraction studies were conducted on polished monolithic and composite extruded samples using Cu-K_α radiation (λ = 1.5406 Å) with a scan speed of 2°/min in an automated Shimadzu LAB-X XRD-6000 diffractometer to determine the phases present. The values of lattice spacing (d) obtained were matched with standard values [18] of phases based on Mg and Al.

2.5. Hardness

Microhardness measurements were made on polished monolithic and composite extruded samples. Vickers microhardness was measured using Matsuzawa MXT50 automatic digital microhardness tester using 25-gf indenting load and 15 s dwell time.

2.6. Tensile testing

Smooth bar tensile properties of the monolithic and composite extruded samples were determined based on ASTM E8M-05. Round tension test samples of 5-mm diameter and 25-mm gauge length were subjected to tension using an MTS 810 machine equipped with an axial extensometer with a crosshead speed set at 0.254 mm/min. Fractography was performed on the tensile fracture surfaces using Hitachi S4300 FESEM.

3. Results and discussion

3.1. Synthesis of monolithic AZ31 and AZ31/Al_2O_3 composites

Synthesis of monolithic and composite materials, the final form being extruded rods, was successfully accomplished with: (a) no detectable metal oxidation, (b) no detectable reaction between graphite crucible and melts. The inert atmosphere used during DMD was effective in preventing oxidation of the Mg melt. No stable carbides of Mg or Al formed due to reaction with the graphite crucible.

3.2. Macrostructural characteristics

No macropores or shrinkage cavities were observed in the cast monolithic and composite materials. No macrostructural defects were observed for extruded rods of monolithic and composite materials.

3.3. Microstructural characteristics

Microstructural analysis results revealed no significant change in grain characteristics of each composite compared to monolithic material as shown in Table 1. Also, there was no significant difference in grain characteristics and Al_2O_3 reinforcement distribution between the fresh and remelted forms of each AZ31/Al_2O_3 composite (see Fig. 1).

In the case of AZ31/1.5 vol% Al_2O_3 (50 nm), the reinforcement distribution was relatively more uniform compared to both AZ31/5.0 vol% Al_2O_3 (300 nm) and AZ31/10.0 vol% Al_2O_3 (1000 nm), where Al_2O_3 agglomerates were observed.

Considering remelted AZ31/1.5 vol% Al_2O_3 (50 nm), the relatively more uniform distribution of Al_2O_3 nanoparticles can be attributed to: (a) minimal gravity-associated segregation due to judicious selection of stirring parameters [9], (b) good wetting of Al_2O_3 nanoparticles by the alloy matrix [19–21], (c) argon gas disintegration of metallic stream [22], and (d) dynamic deposition of composite slurry on substrate followed by hot extrusion.

3.4. X-ray diffraction studies

X-ray diffraction (XRD) results of extruded composite material are shown in Fig. 2. β-$Al_{12}Mg_{17}$ and Al_2O_3 were present in all composites [11,12]. In the case of AZ31/1.5 vol% Al_2O_3 (50 nm), the content of Al_2O_3 nanoparticles was too low (<2.0 vol%) and the Al_2O_3 nanoparticles were relatively more uniformly distributed, making detection by XRD impossible [11,12]. MgO was present in both AZ31/5.0 vol% Al_2O_3 (300 nm) and AZ31/10.0 vol% Al_2O_3 (1000 nm). Accordingly, if MgO was present in AZ31/1.5 vol% Al_2O_3 (50 nm) due to reaction between Mg (in AZ31) and Al_2O_3, its content would be too low and the MgO would be relatively more uniformly distributed in the form of nanoparticles also, making detection by XRD impossible again [11,12].

3.5. Hardness

The results of microhardness measurements are listed in Table 2. The composites exhibited significantly higher hardness (up to +103%) compared to the monolithic material. However, there was no significant difference in hardness between the fresh and remelted forms of each AZ31/Al_2O_3 composite.

In particular, fresh AZ31/5.0 vol% Al_2O_3 (300 nm) and fresh AZ31/10.0 vol% Al_2O_3 (1000 nm) exhibited higher hardness (up to +51%) compared to fresh AZ31/1.5 vol% Al_2O_3 (50 nm). This can be attributed to higher (up to +567%) Al_2O_3 particle content. However, fresh AZ31/5.0 vol% Al_2O_3 (300 nm) exhibited 10% higher hardness than AZ31/10.0 vol% Al_2O_3 (1000 nm) despite having only half the Al_2O_3 particle content. This can be attributed to AZ31/5.0 vol% Al_2O_3 (300 nm) ideally having 67% higher matrix–particle interface area than AZ31/10.0 vol% Al_2O_3 (1000 nm) as listed in Table 3, taking into account MgO formation (see Fig. 2) at the matrix–particle interface. Even though fresh AZ31/1.5 vol% Al_2O_3 (50 nm) has

Table 1
Results of grain size of AZ31 and AZ31/Al_2O_3 composites.

Material	Grain characteristics[a]	
	Size (μm)	Aspect ratio
AZ31	4.0 ± 0.9	1.4
AZ31/1.5 vol% Al_2O_3 (50 nm) fresh	3.1 ± 0.3	1.1
AZ31/1.5 vol% Al_2O_3 (50 nm) remelt	2.7 ± 0.3	1.2
AZ31/5.0 vol% Al_2O_3 (300 nm) fresh	2.6 ± 0.8	1.4
AZ31/5.0 vol% Al_2O_3 (300 nm) remelt	2.7 ± 0.8	1.4
AZ31/10.0 vol% Al_2O_3 (1000 nm) fresh	2.7 ± 0.8	1.4
AZ31/10.0 vol% Al_2O_3 (1000 nm) remelt	2.6 ± 0.8	1.4

[a] Based on approximately 100 grains.

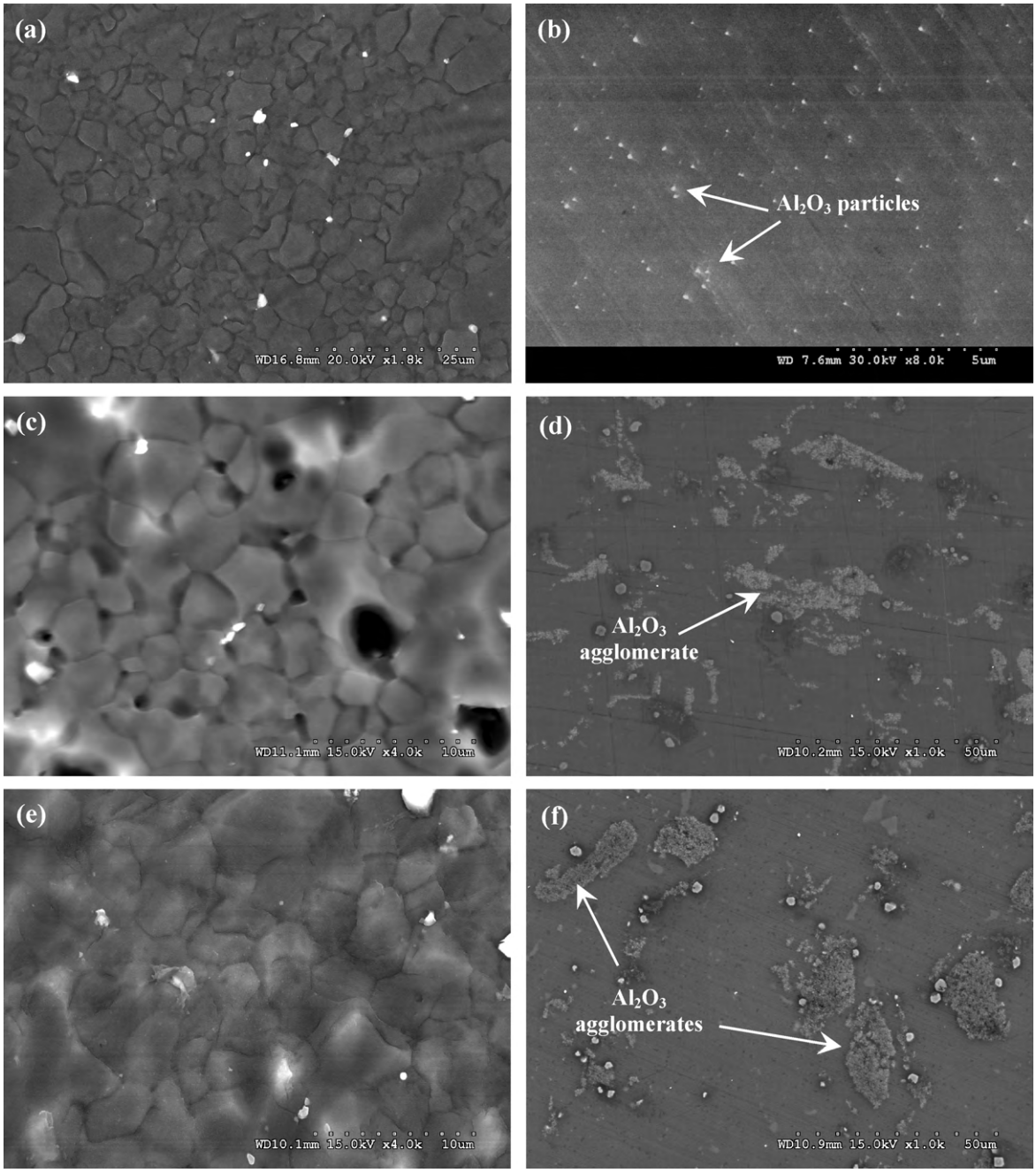

Fig. 1. Representative micrographs showing grain size (left) and Al_2O_3 reinforcement distribution (right) in: (a, b) AZ31/1.5 vol% Al_2O_3 (50 nm), (c, d) AZ31/5.0 vol% Al_2O_3 (300 nm) and (e, f) AZ31/10.0 vol% Al_2O_3 (1000 nm). In each case of AZ31/Al_2O_3 composite, the grain size and Al_2O_3 reinforcement distribution of fresh and remelted forms were similar.

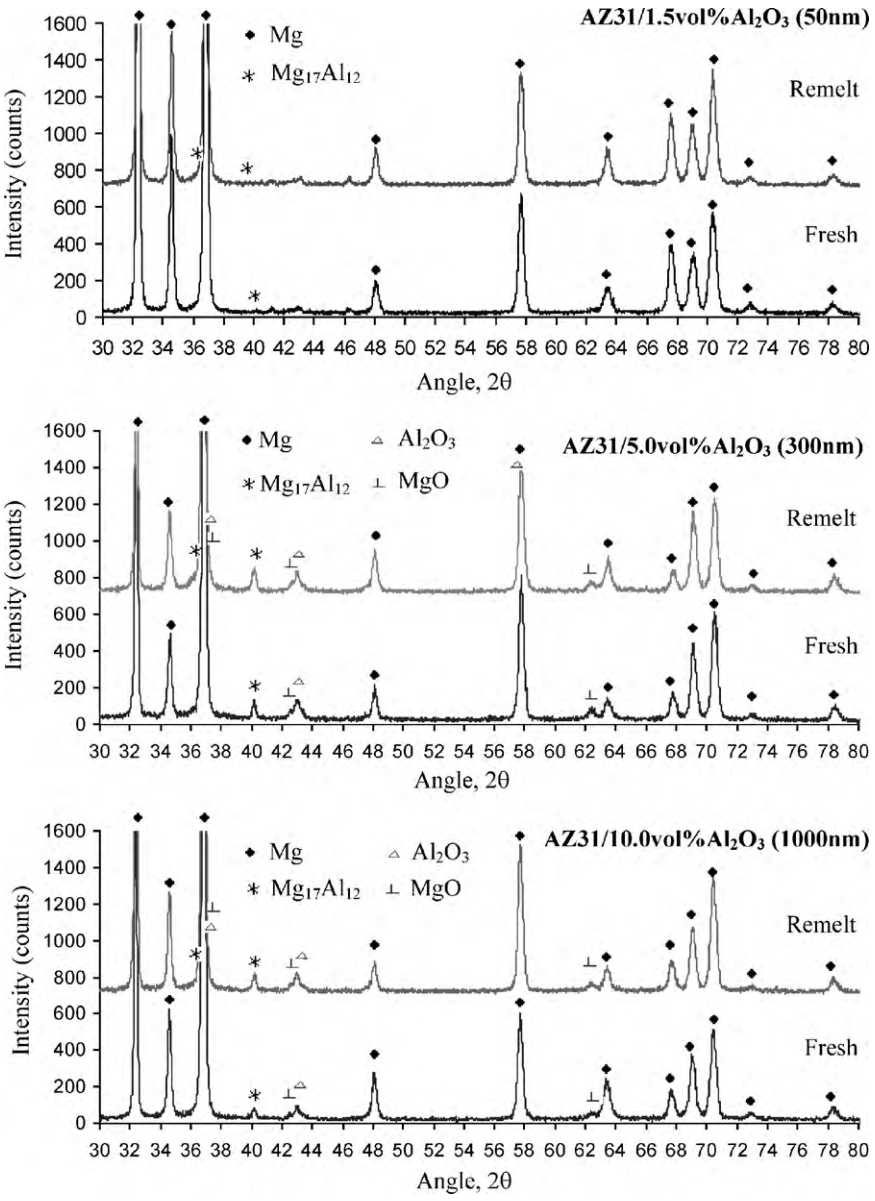

Fig. 2. Representative XRD scans of fresh/remelted: (a) AZ31/1.5 vol% Al_2O_3 (50 nm), (b) AZ31/5.0 vol% Al_2O_3 (300 nm) and (c) AZ31/10.0 vol% Al_2O_3 (1000 nm).

higher (up to +200%) matrix–particle interface area than the other fresh AZ31/Al_2O_3 composites, the relatively low Al_2O_3 particle content of 1.5 vol% is insufficient to increase the hardness of AZ31 to or beyond that of the other fresh AZ31/Al_2O_3 composites.

A significant increase in microhardness by 42% was observed in remelted AZ31/1.5 vol% Al_2O_3 (50 nm) when compared to monolithic material. This was consistent with earlier observations made on Mg/Al_2O_3, AZ31/C_{60} and AZ31/MWCNT nanocomposites [2,3,23–25]. The increase in hardness of the remelted nanocomposite in the present study can be attributed to: (a) intermetallic particles of lower size and roundness ratio in the matrix, (b) relatively more uniform distribution of harder oxide nanoparticles in the matrix, and (c) higher constraint to localized matrix deformation during indentation due to the presence of intermetallic particles (having lower size and roundness ratio) and nanoparticles [8,11,12,23,24].

Table 2
Results of mechanical testing of AZ31 and AZ31/Al_2O_3 composites.

Material	Microhardness (HV)	0.2% TYS (MPa)	UTS (MPa)	Failure strain (%)	WOF (MJ/m^3)[a]
AZ31	64 ± 4	172 ± 15	263 ± 12	10.4 ± 3.9	26 ± 9
AZ31/1.5 vol% Al_2O_3 (50 nm) fresh	86 ± 3	219 ± 4	308 ± 5	14.5 ± 0.7	42 ± 3
AZ31/1.5 vol% Al_2O_3 (50 nm) remelt	91 ± 4	225 ± 3	313 ± 4	14.0 ± 1.0	43 ± 3
AZ31/5.0 vol% Al_2O_3 (300 nm) fresh	130 ± 4	216 ± 3	291 ± 1	3.8 ± 0.6	11 ± 2
AZ31/5.0 vol% Al_2O_3 (300 nm) remelt	124 ± 5	215 ± 4	294 ± 5	2.8 ± 0.4	8 ± 1
AZ31/10.0 vol% Al_2O_3 (1000 nm) fresh	118 ± 6	216 ± 3	293 ± 4	5.5 ± 0.3	16 ± 1
AZ31/10.0 vol% Al_2O_3 (1000 nm) remelt	110 ± 5	215 ± 7	293 ± 8	4.3 ± 0.8	12 ± 2

[a] Obtained from engineering stress–strain diagram using EXCEL software.

Table 3
Al_2O_3 particle characteristics in 1 cc of AZ31/Al_2O_3 composite.

Al_2O_3 particle size (nm)	Al_2O_3 particle volume (cc)[a]	Al_2O_3 particle characteristics in 1 cc of AZ31/Al_2O_3 composite[a]			
		Particle content (vol%)	Volume occupied (cc)	Number of particles	AZ31/Al_2O_3 interface area (m^2)
50	6.55×10^{-17}	1.5	0.015	2.29×10^{14}	1.8
300	1.41×10^{-14}	5.0	0.050	3.54×10^{12}	1.0
1000	5.24×10^{-13}	10.0	0.100	1.91×10^{12}	0.6

[a] Al_2O_3 particles assumed to be spherical and uniformly distributed in the AZ31 matrix.

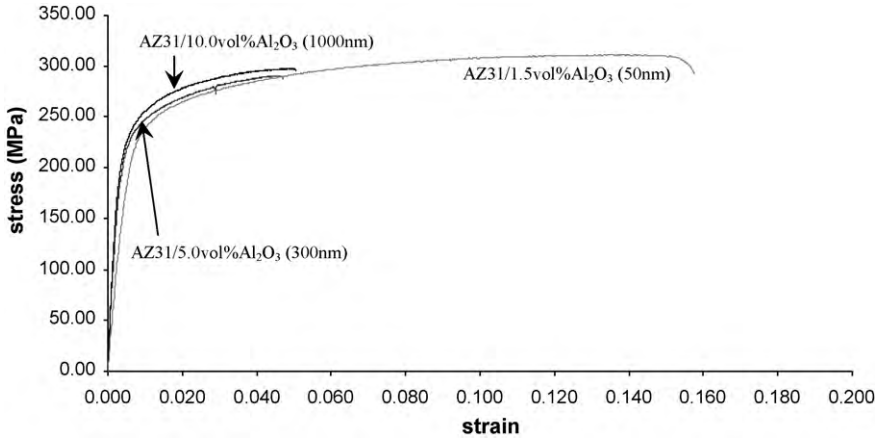

Fig. 3. Representative tensile stress–strain curves of fresh/remelted: (a) AZ31/1.5 vol% Al_2O_3 (50 nm), (b) AZ31/5.0 vol% Al_2O_3 (300 nm) and (c) AZ31/10.0 vol% Al_2O_3 (1000 nm). In each case of AZ31/Al_2O_3 composite, the curves of fresh and remelted forms are similar.

3.6. Tensile behavior

3.6.1. Strength

The overall results of ambient temperature tensile testing of the extruded materials are shown in Table 2 and Fig. 3. The strength of fresh AZ31/1.5 vol% Al_2O_3 (50 nm), fresh AZ31/5.0 vol% Al_2O_3 (300 nm) and fresh AZ31/10.0 vol% Al_2O_3 (1000 nm) was significantly higher (up to +27%) compared to monolithic AZ31. However, there was no significant difference in strength between the fresh and remelted forms of each AZ31/Al_2O_3 composite.

Specifically, compared to fresh AZ31/5.0 vol% Al_2O_3 (300 nm) and fresh AZ31/10.0 vol% Al_2O_3 (1000 nm), the strength increment of fresh AZ31/1.5 vol% Al_2O_3 (50 nm) over that of monolithic AZ31 was slightly higher by +2%. This was so despite the significantly lower (up to −85%) Al_2O_3 particle content. This indicated the relatively potent AZ31 strengthening effect of Al_2O_3 reinforcement when in the form of nanoparticles.

In the case of remelted AZ31/1.5 vol% Al_2O_3 (50 nm), the strength was significantly increased (+31%) compared to monolithic AZ31. This can be attributed to well-known factors (pertaining

Table 4
Comparison of tensile properties of magnesium based materials.

Material	0.2% TYS (MPa)	UTS (MPa)	Failure strain/elongation (%)	WOF (MJ/m^3)[a]
AZ31/1.5 vol% Al_2O_3 (50 nm) fresh	**219 ± 4**	**308 ± 5**	**14.5 ± 0.7**	**42 ± 3**
AZ31/1.5 vol% Al_2O_3 (50 nm) remelt	**225 ± 3**	**313 ± 4**	**14.0 ± 1.0**	**43 ± 3**
Extruded AZ31B/C-F [30]	200	255	12	–
Extruded AZ61A-F [30]	**205**	**305**	**16**	–
Extruded AZ91D[b,c] [31,32]	215	296	10.2	–
Extruded AZ91D[b,d] [32]	**226**	**313**	**15.6**	–
Extruded ZK21A-F [30]	195	260	4	–
Extruded ZK31-T5 [30]	210	295	7	–
Extruded ZK40A-T5 [30]	255	275	4	–
Sand cast AZ63A-T6 [30]	130	275	5	–
Sand cast AZ81A-T4 [30]	83	275	15	–
Sand cast AZ91C/E-T6 [30]	145	275	6	–
Sand cast AZ92A-T6 [30]	150	275	3	–
Sand cast ZK61A-T5 [30]	185	310	–	–
Sand cast ZK61A-T6 [30]	195	310	10	–
Extruded Mg/0.22 vol% Y_2O_3[b,e] [33]	218 ± 2	277 ± 5	12.7 ± 1.3	29.6 ± 3.5
Extruded Mg/0.66 vol% Y_2O_3[b,e] [33]	312 ± 4	318 ± 2	6.9 ± 1.6	18.2 ± 4.7
Extruded Mg/1.11 vol% Al_2O_3[b,e] [29]	175 ± 3	246 ± 3	14.0 ± 2.4	31.7 ± 6.3
Extruded AZ91D/15 vol% SiCp[b,c,f] [31]	257	289	0.7	–
Extruded AZ91D/15 vol% SiCp[b,d,f] [31]	205	233	1.1	–

[a] Obtained from engineering stress–strain diagram using EXCEL software.
[b] Hot extruded at 250 °C.
[c] Rheocast material prior to extrusion.
[d] Die-cast material prior to extrusion.
[e] Nano-size reinforcement.
[f] Micro-size reinforcement.

to reinforcement) such as: (a) dislocation generation due to elastic modulus mismatch and coefficient of thermal expansion mismatch between the matrix and reinforcement [8,23,26,27], (b) Orowan strengthening mechanism (inclusive of reduction in diameter of intermetallic particles) [26–30] and (c) load transfer from matrix to reinforcement [23,26]. The strength of remelted AZ31/1.5 vol% Al_2O_3 (50 nm) was similar to or better than: (a) selected wrought/cast Zr-free (or Al-containing) Mg alloys having similar or higher Al content, (b) selected wrought/cast Zr-containing (or Al-free) Mg alloys, (c) selected wrought Mg nanocomposites (extruded at lower temperature) and (d) selected wrought Zr-free (or Al-containing) Mg alloy microcomposites having higher Al content, as listed in Table 4 [29–33].

3.6.2. Failure strain

The overall results of ambient temperature tensile testing of the extruded materials are shown in Table 2 and Fig. 3. The failure strain of fresh AZ31/5.0 vol% Al_2O_3 (300 nm) and fresh AZ31/10.0 vol% Al_2O_3 (1000 nm) was significantly lower (up to −63%) compared to monolithic AZ31. However, the failure strain of fresh AZ31/1.5 vol% Al_2O_3 (50 nm) was significantly higher (+39%) compared to monolithic AZ31. There was no significant difference in failure strain between the fresh and remelted forms of each AZ31/Al_2O_3 composite.

Compared to fresh AZ31/5.0 vol% Al_2O_3 (300 nm) and fresh AZ31/10.0 vol% Al_2O_3 (1000 nm), the failure strain change of fresh AZ31/1.5 vol% Al_2O_3 (50 nm) alone over that of monolithic AZ31 was significantly positive (+39%). This was so despite the significantly lower (up to −85%) Al_2O_3 particle content. This indicated the unique AZ31 ductility enhancing effect of Al_2O_3 reinforcement when in the form of nanoparticles.

Considering remelted AZ31/1.5 vol% Al_2O_3 (50 nm), the failure strain was significantly increased (+35%) compared to monolithic AZ31. This can be attributed to the following factors (pertaining to reinforcement): (a) presence and relatively more uniform distribution of ceramic nanoparticles (see Fig. 1) [11,12,24,33] and (b) reduction in size and roundness ratio of intermetallic particles [8,11,12,34]. In the case of relatively more uniform distribution of ceramic nanoparticles, it has been shown in previous studies that the nanoparticles provide sites where cleavage cracks are opened ahead of the advancing crack front. This: (1) dissipates the stress concentration which would otherwise exist at the crack front and (2) alters the local effective stress state from plane strain to plane stress in the neighbourhood of crack tip [11,12,24,33]. In the case of reduction in size and roundness ratio of intermetallic particles, roundness is a measure of the sharpness of a particle's edges and corners. The rounder the particle, the lower the extent of stress localization around the particle in the matrix. Breakdown of the intermetallic particles located at grain boundaries and the change in their distribution from a predominantly aggregated type to dispersed type can assist in improving ductility [8,11,12,34]. The more the intermetallic particles are dispersed, the lower the presence of voids between the particles (aggregates are generally void-filled in comparison).

The failure strain of remelted AZ31/1.5 vol% Al_2O_3 (50 nm) was similar to or better than: (a) selected wrought/cast Zr-free (or Al-containing) Mg alloys having similar or higher Al content, (b) selected wrought/cast Zr-containing (or Al-free) Mg alloys, (c) selected wrought Mg nanocomposites (extruded at lower temperature) and (d) selected wrought Zr-free (or Al-containing) Mg alloy microcomposites having higher Al content, as listed in Table 4 [29–33]. Tensile fracture behavior of composite material was mixed (ductile + brittle) as shown in Fig. 4. However, the tensile fractured surface of fresh/remelted AZ31/1.5 vol% Al_2O_3 (50 nm) had (a) higher occurrence of smaller dimple-like features and (b) absence of microcracks, compared to that of

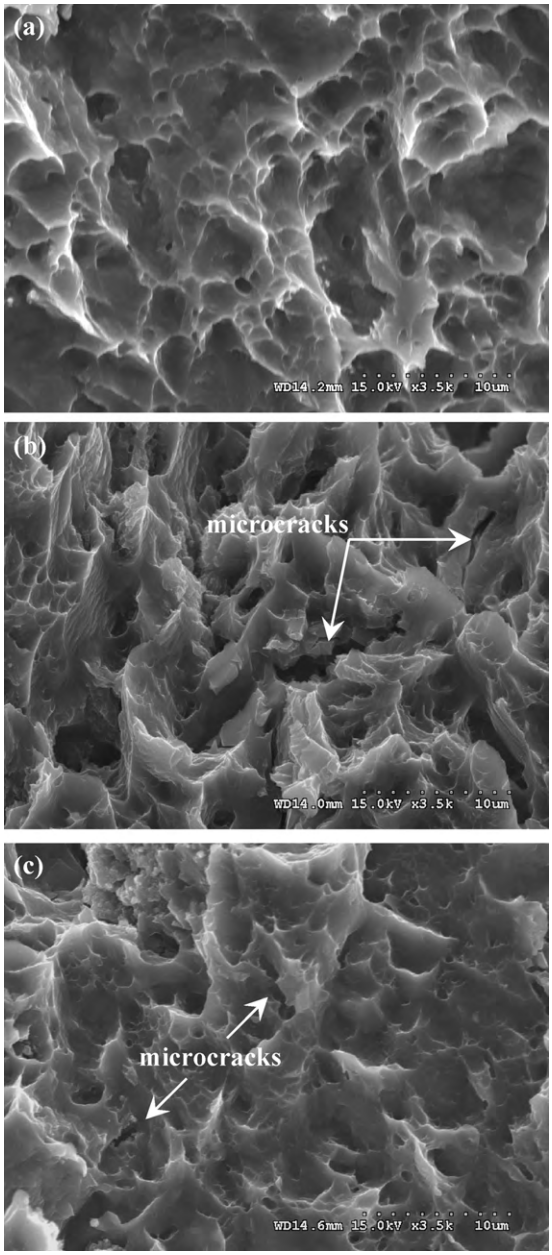

Fig. 4. Representative FESEM micrographs showing tensile fracture surfaces of fresh/remelted: (a) AZ31/1.5 vol% Al_2O_3 (50 nm), (b) AZ31/5.0 vol% Al_2O_3 (300 nm) and (c) AZ31/10.0 vol% Al_2O_3 (1000 nm). In each case of AZ31/Al_2O_3 composite, the fracture surfaces of fresh and remelted forms are similar.

fresh/remelted AZ31/5.0 vol% Al_2O_3 (300 nm) and fresh/remelted AZ31/10.0 vol% Al_2O_3 (1000 nm). The tensile cavitation resistance was lower and the microcrack formation resistance was higher in the fresh/remelted AZ31/Al_2O_3 nanocomposite compared to the other fresh/remelted AZ31/Al_2O_3 composites.

3.6.3. Work of fracture

The tensile work of fracture (WOF) of monolithic material and composites is listed in Table 2 and illustrated in Fig. 3. WOF quantified the ability of the material to absorb energy up to fracture under load [35]. The WOF of fresh AZ31/5.0 vol% Al_2O_3 (300 nm) and fresh AZ31/10.0 vol% Al_2O_3 (1000 nm) was significantly lower (up to −58%) compared to monolithic AZ31. However, the WOF of fresh AZ31/1.5 vol% Al_2O_3 (50 nm) was significantly higher (+62%) compared to monolithic AZ31. There was no significant difference

in WOF between the fresh and remelted forms of each AZ31/Al_2O_3 composite.

Compared to fresh AZ31/5.0 vol% Al_2O_3 (300 nm) and fresh AZ31/10.0 vol% Al_2O_3 (1000 nm), the WOF change of fresh AZ31/1.5 vol% Al_2O_3 (50 nm) alone over that of monolithic AZ31 was significantly positive (+62%). This was so despite the significantly lower (up to −85%) Al_2O_3 particle content. This indicated the unique AZ31 WOF enhancing effect of Al_2O_3 reinforcement when in the form of nanoparticles.

Considering remelted AZ31/1.5 vol% Al_2O_3 (50 nm), the WOF was significantly increased (+65%) compared to monolithic AZ31. The significantly high increment in WOF exhibited by remelted AZ31/1.5 vol% Al_2O_3 (50 nm) shows its potential to be used in damage tolerant design to a similar extent compared to wrought Zr-free (or Al-containing) Mg alloys having significantly higher Al content such as extruded AZ61A-F and extruded AZ91D as indicated in Table 4 (in bold) [30,32]. Compared to these two extruded alloys, the strength and failure strain of remelted AZ31/1.5 vol% Al_2O_3 (50 nm) is similar, implying that the WOF is also similar among these materials.

4. Conclusions

Monolithic AZ31 and AZ31/Al_2O_3 composites individually containing 50 nm, 300 nm or 1000 nm sized Al_2O_3 particles can be successfully synthesized on a fresh/remelt basis using the DMD technique followed by hot extrusion.

There was no significant difference in strength between the fresh and remelted forms of each AZ31/Al_2O_3 composite. In the case of remelted AZ31/1.5 vol% Al_2O_3 (50 nm), the strength was increased the most (+31%) compared to monolithic AZ31.

There was no significant difference in failure strain between the fresh and remelted forms of each AZ31/Al_2O_3 composite. Considering remelted AZ31/1.5 vol% Al_2O_3 (50 nm), the failure strain change was significantly positive (+35%) compared to monolithic AZ31, unlike that of remelted AZ31/Al_2O_3 composites containing larger sized (300 nm or 1000 nm) Al_2O_3 particles which were significantly negative (up to −73%).

There was no significant difference in WOF between the fresh and remelted forms of each AZ31/Al_2O_3 composite. Considering remelted AZ31/1.5 vol% Al_2O_3 (50 nm), the WOF was significantly increased (+65%) compared to monolithic AZ31, unlike that of remelted AZ31/Al_2O_3 composites containing larger sized (300 nm or 1000 nm) Al_2O_3 particles which were significantly decreased (up to −69%).

Acknowledgements

Authors wish to acknowledge National University of Singapore for funding this research through grants and studentships, and Agency for Science, Technology and Research (ASTAR) Grant 092 137 0015 (WBS# R-265-000-321-305).

References

[1] Y. Morisada, H. Fujii, T. Nagaoka, M. Fukusumi, Mater. Sci. Eng. A 433 (2006) 50–54.
[2] Y. Morisada, H. Fujii, T. Nagaoka, M. Fukusumi, Scripta Mater. 55 (2006) 1067–1070.
[3] Y. Morisada, H. Fujii, T. Nagaoka, M. Fukusumi, Mater. Sci. Eng. A 419 (2006) 344–348.
[4] W.B. Ding, H.Y. Jiang, X.Q. Zeng, D.H. Li, S.S. Yao, Appl. Surf. Sci. 253 (2007) 3877–3883.
[5] W. Ding, H. Jiang, X. Zeng, D. Li, S. Yao, Mater. Lett. 61 (2007) 496–501.
[6] D. Wenbin, J. Haiyan, Z. Xiaoqin, L. Dehui, Y. Shoushan, J. Alloys Compd. 429 (2007) 233–241.
[7] K. Mizuuchi, K. Inoue, K. Hamada, M. Sugioka, M. Itami, M. Fukusumi, M. Kawahara, Mater. Sci. Eng. A 367 (2004) 343–349.
[8] M. Paramsothy, S.F. Hassan, N. Srikanth, M. Gupta, J. Nanosci. Nanotechnol. 10 (2010) 956–964.
[9] L.M. Tham, M. Gupta, L. Cheng, Mater. Sci. Technol. 15 (1999) 1139–1146.
[10] M. Gupta, M.O. Lai, S.C. Lim, J. Alloys Compd. 260 (1997) 250–255.
[11] Q.B. Nguyen, M. Gupta, J. Alloys Compd. 459 (2007) 244–250.
[12] M. Paramsothy, S.F. Hassan, N. Srikanth, M. Gupta, Mater. Sci. Eng. A 527 (2009) 162–168.
[13] P. Rohatgi, J. Met. 43 (1991) 10–15.
[14] D.J. Lloyd, Int. Mater. Rev. 39 (1994) 1–23.
[15] I.A. Ibrahim, F.A. Mohamed, E.J. Lavernia, J. Mater. Sci. 26 (1991) 1137–1156.
[16] T.W. Clyne, P.J. Withers, An Introduction to Metal Matrix Composites, Cambridge University Press, Cambridge, 1993.
[17] D.M. Schuster, M.D. Skibo, R.S. Bruski, R. Provencher, G. Riverin, J. Met. 45 (1993) 26–30.
[18] International Centre for Diffraction Data, Powder Diffraction File, Pennsylvania, 1991.
[19] B.Q. Han, D.C. Dunand, Mater. Sci. Eng. A 277 (2000) 297–304.
[20] N. Eustathopoulos, M.G. Nicholas, B. Drevet, Wettability at High Temperatures, in: Pergamon Materials Series, vol. 3, Pergamon, New York, 1999.
[21] J.D. Gilchrist, Extraction Metallurgy, third ed., Pergamon Press, New York, 1989.
[22] M. Gupta, M.O. Lai, C.Y. Soo, Mater. Sci. Eng. A 210 (1996) 114–122.
[23] S.F. Hassan, M. Gupta, J. Mater. Sci. 41 (2006) 2229–2236.
[24] S.F. Hassan, M. Gupta, J. Alloys Compd. 419 (2006) 84–90.
[25] S.F. Hassan, M. Gupta, Metall. Mater. Trans. A 36 (8) (2005) 2253–2258.
[26] Z. Szaraz, Z. Trojanova, M. Cabbibo, E. Evangelista, Mater. Sci. Eng. A 462 (2007) 225–229.
[27] L.H. Dai, Z. Ling, Y.L. Bai, Compos. Sci. Technol. 61 (2001) 1057–1063.
[28] D. Hull, D.J. Bacon, Introduction to Dislocations, fourth ed., Butterworth-Heinemann, Oxford, 2002, pp. 43, 231.
[29] S.F. Hassan, M. Gupta, Compos. Struct. 72 (2006) 19–26.
[30] M.M. Avedesian, H. Baker, ASM Specialty Handbook: Magnesium and Magnesium Alloys, ASM International®, Ohio, 1999, pp. 12–25, 165–172, 226–248, 258–263.
[31] V. Laurent, P. Jarry, G. Regazzoni, D. Apelian, J. Mater. Sci. 27 (1992) 4447–4459.
[32] A. Tissier, D. Apelian, G. Regazzoni, J. Mater. Sci. 25 (1990) 1184–1196.
[33] S.F. Hassan, M. Gupta, J. Alloys Compd. 429 (2007) 176–183.
[34] G.E. Dieter, Mechanical Metallurgy, SI Metric ed., McGraw-Hill Book Company, London, 1988.
[35] R.E. Reed-Hill, Physical Metallurgy Principles, second ed., D Van Nostrand Company, USA, 1964, pp. 192, 267, 725.